Earthquakes and Structures, *Vol. 12, No. 5 (2017) 489-499*
DOI: https://doi.org/10.12989/eas.2017.12.5.489

Seismic vulnerability assessment of confined masonry buildings based on ESDOF

Fariman Ranjbaran* and Amir Reza Kiyani

Civil Engineering Department, Islamshahr Branch of the Islamic Azad University (IAU), Islamshahr, Tehran, Iran

(Received December 26, 2015, Revised April 10, 2017, Accepted April 14, 2017)

Abstract. The effects of past earthquakes have demonstrated the seismic vulnerability of confined masonry structures (CMSs) to earthquakes. The results of experimental analysis indicate that damage to these structures depends on lateral displacement applied to the walls. Seismic evaluation lacks an analytical approach because of the complexity of the behavior of this type of structure; an empirical approach is often used for this purpose. Seismic assessment and risk analysis of CMSs, especially in area have a large number of such buildings is difficult and could be riddled with error. The present study used analytical and numerical models to develop a simplified nonlinear displacement-based approach for seismic assessment of a CMS. The methodology is based on the concept of ESDOF and displacement demand and is compared with displacement capacity at the characteristic period of vibration according to performance level. Displacement demand was identified using the nonlinear displacement spectrum for a specified limit state. This approach is based on a macro model and nonlinear incremental dynamic analysis of a 3D prototype structure taking into account uncertainty of the mechanical properties and results in a simple, precise method for seismic assessment of a CMS. To validate the approach, a case study was considered in the form of an analytical fragility curve which was then compared with the precise method.

Keywords: confined masonry; displacement based assessment; fragility curves; vulnerability assessment; performance based; analytical model; OpenSees; ESDOF

1. Introduction

Confined masonry structures (CMSs) exist or are built as private or public buildings. This kind of structure consists of masonry walls (clay brick or concrete block) accompanied by vertical and horizontal tie elements (steel or concrete) on its four sides. Reasons for the construction of a CMS include easy access to low-cost materials and the simple technology required for construction.

The masonry walls bear most of the vertical and lateral loads and the tie elements provide ductility for walls against seismic loading. Past experience has demonstrated that CMSs can be vulnerable to earthquakes. In addition to the poor quality of construction, the lack of proper modeling and analysis of CMS against seismic loading to determine its capacity and demand is the reason for this vulnerability.

A CMS is often constructed based on experimental studies because of the difficulty and complexity of modeling the confined masonry walls. Previous investigation has shown that it is possible to model a CMS for the purpose of risk analysis using a numerical method (Riahi *et al*. 2009, Flores and Alcocer 1996, Teran-Gilmore *et al*. 2009, Moroni *et al*. 1994, Tomazevic and Klemenc 1998, Ranjbaran *et al*. 2012), especially when there are a considerable number of CMSs in an area, It is time-consuming and requires much effort to create such a model.

*Corresponding author, Assistant Professor
E-mail: ranjbaran_far@iiau.ac.ir

Using the design of structures to achieve a specified performance limit state as defined by drift limits and equivalent single degree of freedom (ESDOF), it is possible to assess a structure subjected to earthquake loading based on displacement in the simplified method (Priestley *et al*. 2007, Priestley 1997). Previous investigations have indicated that damage to CMSs depends on lateral displacement applied to the walls (Ruiz-Garcia and Negrete 2009, Ranjbaran and Hosseini 2014). This means that it should be possible to use performance and limit states for assessment of CMS performance during earthquakes. By estimation of the peak roof inelastic drift demand of CMS and deformation capacity and comparing with each other, it is possible the seismic evaluation of this type of structures in the simple procedure. ESDOF could be used for this purpose. Differences exist among proposed procedures to calculate of demand displacement. For example the inelastic displacement ratio and elastic displacement spectra, the coefficient method established in several FEMA documents or equivalent linearization approach with secant stiffness and equivalent viscous damping ratio for a given level of displacement ductility demand were proposed for this purpose (Ruiz-Garcia and Negrete 2009, Teran-Gilmore *et al*. 2009, Priestley 1997).The proposed procedures could be very useful for obtaining rapid estimates of expected performance during future earthquake events and for assessing the seismic vulnerability of regular confined masonry structures.

The procedure developed in Priestley (1997) was used in this study in the form of a simplified method for assessment of confined masonry structures subject to

http://www.techno-press.com/journals/eas&subpage=7
ISSN: 2092-7614 (Print), 2092-7622 (Online)

earthquake loading based on displacement. This method calculates the demand and capacity displacement ratio (DCR) using the specified drift limit (performance limit) and the ESDOF equivalent to the actual building (Ahamad *et al*. 2010). If the DCR>1, the building is considered vulnerable to earthquakes, otherwise it is invulnerable. The proposed method was achieved by modeling a 3D prototype structure with a common plan and varying the mechanical and geometrical properties using OpenSees software (OpenSees 2006, 2009).

Analysis was based on nonlinear incremental dynamic analysis (IDA) and macro-modeling of the prototype structure. The analytical and macro-models were analyzed for the CMS using numerical modeling of confined masonry walls and the results validated the experimental models (Fig. 1) (Ranjbaran and Hosseini 2014). Each bearing element of the CMS (masonry wall with tie elements) was modeled as a linear element in a macro-model with geometrical properties similar to those of masonry walls. The nonlinear behavior of a confined masonry wall (after crack behavior) was modeled by a shear hinge at the mid-span of the macro-model showing characteristic behavior. The cyclic behavior of the macro-model was captured by the proposed analytical model in the form of a backbone curve and thin Takeda-type hysteretic behavior where stiffness of unloading decreased with an increase in displacement (Ranjbaran and Hosseini 2014).

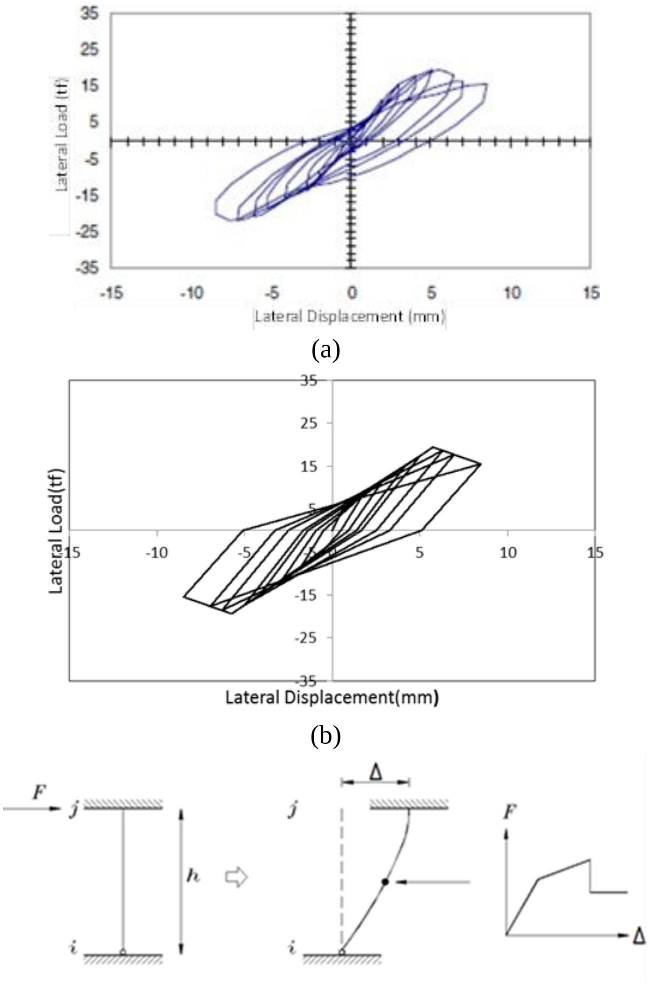

Fig. 1 Comparison between experimental and numerical models related to the masonry wall with confinement: a) Experimental model by Marinilli (Marinilli and Castilla 2004), b)Numerical model (Ranjbaran and Hosseini 2014), c) The proposed macro model for confined masonry wall (Ranjbaran *et al*. 2012)

2. Methodology of displacement-based seismic assessment

Displacement-based seismic assessment of a structure was based on ESDOF was proposed by Shibata and Sozen (Shibata and Sozen 1976). In this approach, the actual nonlinear behavior of a building is idealized using an ESDOF linear system with a bilinear force-displacement response (Fig. 2). In Fig. 2, H_T is the total height, h_i and Δ_i are the ith floor height and lateral displacement for a given displaced shape, respectively, m_i is the floor mass, M_e and H_e are the equivalent mass and height of the ESDOF system, respectively, Δ_y and Δ_{LS} are the equivalent yield and limit state displacement (corresponding to drift limit in actual building) of the ESDOF, respectively. This value represents the displacement capacity of the actual building at the center of the seismic force according to a specified deformation shape for an actual building.

K_i and K_{sec} are the initial and secant stiffness, respectively, F_y is the yielding force of the ESDOF, α is the ratio of the post-yield stiffness to the initial stiffness of the ESDOF system and represents a reduction in stiffness and strength of the actual structure caused by the cyclic response with increasing drift demand. For any limit state, the ESDOF system vibrates linearly at the secant period; the secant stiffness and equivalent mass of an actual building with viscous damping represents the equivalent damping of the actual building at the specified limit state. Fig. 3 shows the ESDOF system representing the characteristics of the actual building for equivalent displacement and the actual energy dissipation at the seismic demand. In Fig. 3, θ denotes the drift ratio limit of the actual building and ESDOF system.

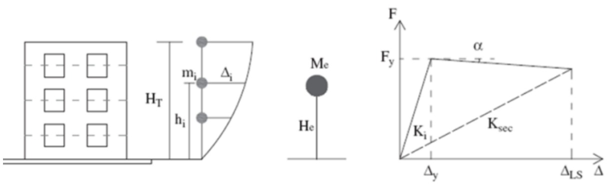

Fig. 2 Single degree of freedom idealization of building (Ahmad *et al*. 2010)

As stated, limit state displacement depends on the specified deformed shape considered for the actual building (Priestley *et al*. 2007). In a multi-story confined masonry building with a rigid diaphragm in the ceiling, earthquake damage is usually concentrated in the first floor of the building (soft story mechanism in the first floor) (Fig. 4) (Ranjbaran *et al*. 2012, Alcocer *et al*. 1996, Design code 2011).

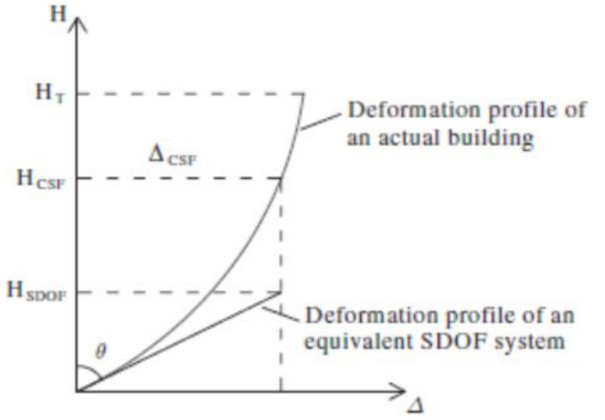

Fig. 3 Displacement of actual building and its representation by ESDOF system (Ahmad *et al*. 2010)

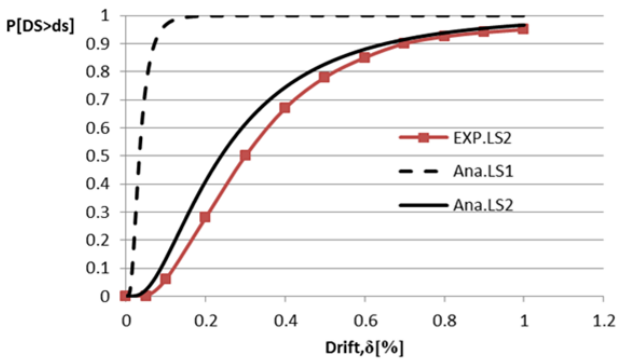

Fig. 5 The drift-based fragility curves corresponding to the maximum strength (LS2) and the elastic limit strength (LS1) for CMWs (Ranjbaran and Hosseini 2014)

This failure mechanism is considered to calculate limit state displacement (Δ_{LS}); Δ_y denotes elastic limit displacement of the building (linear shape of displacement). If a rigid diaphragm in the ceiling and regularity of plan is assumed, θ becomes the drift ratio limit of the masonry wall.

The equivalent yield and limit displacements are formulated using Eqs. (1) to (3) in which H_e is the height of the ESDOF system (H_{SDOF}) (Priestley *et al.* 2007, Ahamad *et al*. 2010, Lang 2002) as

$$\Delta_y = \theta_y H_e \tag{1}$$

$$\Delta_{LS} = \theta_y H_e + (\theta_{LS} - \theta_y) H_1 \tag{2}$$

$$H_e = \frac{\sum h_i\, m_i \varphi_i}{\sum m_i \varphi_i} \tag{3}$$

where H_1 is the height of first floor, θ_y and θ_{LS} are the yielding drift ratio and specified drift ratio of the confined masonry wall, respectively, φ_i is the first mode displacement at the ith floor level normalized such that the first mode displacement at the top story (φ_n) equals 1.

Earlier studies on fragility curves have represented curves as confined masonry walls based on drift ratio for limit states LS1 and LS2 for elastic and maximum limit strength, respectively (Fig. 5) (Ranjbaran and Hosseini 2014). The drift ratios of θ_y and θ_{LS} for LS1 and LS2 are calibrated in Sec. 5. Capacity displacement of the elastic limit and maximum strength displacement of the ESDOF

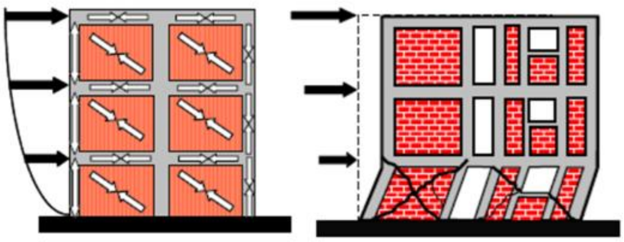

Fig. 4 Soft storey mechanism for multi-storey confined masonry building (Brzev 2007)

can be calculated using Eqs. (1) and (2), respectively. Capacity displacements between those for the specified drift ratio limit can also be determined.

To calculate demand displacement in the ESDOF, the period of ESDOF equivalent to the specified limit state should be specified and the inelastic displacement spectra defined. ESDOF vibrates with the secant stiffness (K_{sec}) or equivalent period (T_{LS}) in the specified limit state.

This parameter can be determined using Eqs. (4) and (5) (Priestley *et al*. 2007, Ahamad *et al*. 2010, Chopra and Goel 2001) as

$$T_{LS} = T_y \sqrt{\frac{\mu_{LS}}{1 + \alpha\mu_{LS} - \alpha}} \tag{4}$$

$$\mu_{LS} = \Delta_{LS}/\Delta_y \tag{5}$$

where μ_{LS} is the ductility of the ESDOF at a specified limit state and T_y is the yield period of vibration. In this study, α and T_y were calibrated from the nonlinear dynamic time-history analysis of the prototype structure.

It is possible to define demand displacement from nonlinear displacement spectra by specifying fundamental vibration periods at different limit states (T_{LS}) for the energy dissipation of the system provided by the actual nonlinear behavior of the buildings. The energy dissipation of the system can be considered by lowering the 5% damped or linear displacement spectra using an appropriate reduction factor as proposed by EC8 (CEN 1994).This factor is calculated in Eq. (6) as

$$\eta = \sqrt{7/(2 + \xi_{eq})} \tag{6}$$

where η is the reduction factor for the elastic displacement spectra and ξ_{eq} is the equivalent viscous damping (%) of the system at a given limit state. In the present study, equivalent damping is the sum of the elastic and hysteretic damping (Priestley *et al*. 2007, Chopra and Goel 2001, Dwairiand *et al*. 2007) expressed in Eq. (7) as

$$\xi_{eq} = \xi_{el} + \xi_{hyst} \tag{7}$$

where ξ_{el} is 5% (Flores and Alcocer 1996, Ranjbaran and

Hosseini 2014, Tomazevich and Klemenk 1997) and ξ_{hyst} is determined by the total energy absorbed during the hysteretic behavior of the substitute structure in response to specific accelerograms (Priestley *et al*. 2007, Dwairi *et al*. 2007, Chopra and Goel 1999). Here, ξ_{hyst} is calibrated by nonlinear dynamic time history analysis of the prototype structure.

Briefly the steps of the method and the required steps for seismic assessment of the structures based on displacement are as follows:

1- Calculation of capacity displacement corresponding to limit state of the structure in its ESDOF system (δ_c). Eqs. (1) and (2) and Fig. 5 can be used for this purpose.

2- Calculation of demand displacement corresponding to limit state of the structure in its ESDOF system (δ_d). By using the reduced elastic displacement spectra as nonlinear displacement spectra and fundamental vibration periods at different limit states, the demand displacement could be calculated. Eqs. (4), (5) and (6) and Fig. 17 can be used for this purpose.

3- If $\delta_c>\delta_d$ the structure is not vulnerable otherwise the structure is vulnerable.

3. Prototype structure

The prototype structure was analyzed for 1, 2 and 3-story CMSs where each story is 3 m in height, composed of clay bricks, and has a rigid diaphragm in the ceiling. The ties were assumed to be concrete in accordance with Iranian Standard #2800. The plan of the building is shown in Fig. 6. The analysis was performed using OpenSees (Ranjbaran and Hosseini 2014, OpenSees 2006). Modeling of the prototype structure was carried out in the form of 3D using the proposed analytical and macro-model developed previously by the authors (Ranjbaran and Hosseini 2010, 2014, Ranjbaran *et al*. 2012). The nonlinear IDA approach was applied to derive the results (Fig. 7).

Each of acceleration record of earthquake was applied to models in main directions of structure.

In the various structural models and in the main direction of structure the steps required for IDA are as follows:

1- All of the selected records (two component records) were scaled to 1 g and then scaled from PGA=0.1 to 1 g at increments of 0.1.

2- The scaled records were applied in the main direction of structure and nonlinear analysis was done.

3- The maximum displacement of the center mass of stories and maximum base shear were determined for each PGA as the maximum demand from each response record.

The tensile strength of the masonry (f_t) is important because it affects features of CMW such as ductility, strength, and mechanical properties (Flores and Alcocer 1996, Ranjbaran *et al*. 2012). This parameter was considered to be a random variable and was varied from 0.04 to 0.25 MPa (E_m=444-2778, G_m=178-1111), which corresponds to cement-sand mortar ratios of 1:12 to 1:6, respectively.

The thickness of the walls was assumed to be 22 cm and the horizontal and vertical ties assigned to the analytical model were assumed to take the form of reinforced concrete with dimensions of 20×20 cm and $f_c' = 15$ MPa, with reinforcement inside ties 4Φ10 and the yielding strength of 300 MPa according to Iranian Standard #2800. It should be mentioned that the tie elements are taken into account in the proposed analytical models in the way that the masonry wall and tie elements are considered together in the proposed macro model, in the other words the proposed analytical models were developed based on the shear behavior of a confined masonry wall (CMW) (Ranjbaran and Hosseini 2010, 2014, Ranjbaran *et al*. 2012).

Table 1 Properties of confined masonry walls

	K[KN/mm]	Qp[KN]	Qu[KN]	Qr[KN]	Du[mm]	Dy[mm]	D=(Du-Dy)/Dy	L[m]
B,1-4	197.68	160.1	210.68	118.47	1.73	0.81	1.13	5
D,1-2	50.04	69.8	91.8	43.6	11.68	1.39	7.38	2.1
A,1-5 A,5-7	158.54	68.6	70.7	39.8	1.82	0.43	3.21	5
D,3-6,D,6-7	126.34	65.7	67.7	39.3	1.75	0.52	2.37	4.4
B,6-7	197.68	180.1	236.92	152.01	0.91	0.91	1.00	5
1,5,7 A-B	94.81	94.8	124.74	61.8	6.71	1.00	5.71	3
1,B-D	197.68	160.1	210.68	118.47	1.73	0.81	1.13	5
3,C-D	151.66	135.0	177.62	97.5	3.38	0.89	2.80	4.1
7,B-D	197.68	147.1	193.56	102.01	2.24	0.74	2.01	5

K: Initial stiffness
$\mathbf{Q_u}$: Maximum resistance
$\mathbf{Q_p}$: Elastic limit resistance
$\mathbf{Q_r}$: Residual resistance
D: Ductility
$\mathbf{D_u}$: Ultimate Displacement
$\mathbf{D_y}$: Yield Displacement
L: Wall length

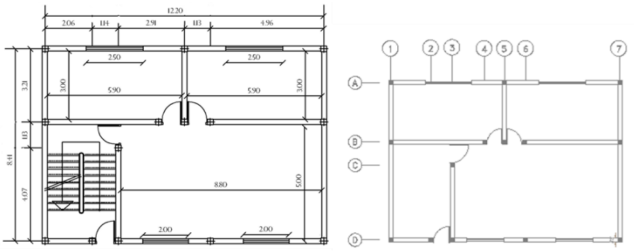

(a) (b)

Fig. 6 Prototype structure: (a) with dimensions; (b) with center line

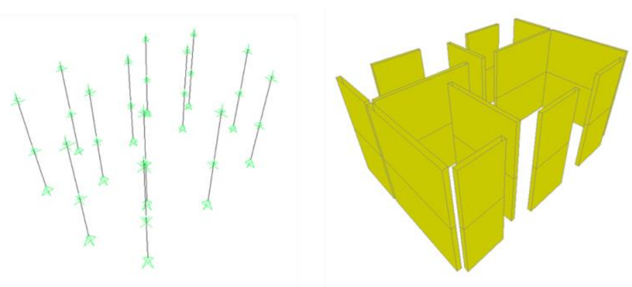

(a) (b)

Fig. 7 3D model of prototype structure: (a) linear element; (b) extruded view

Table 2 Selected earthquake records

Earthquake	Station	Direction	Distance (Km)	Mw	PGA (g)	Peak Fourier Amplitude [HZ]
SAN FERNANDO	24278	E	24.2	6.6	0.32	2.93
		N			0.26	2.15
VICTORIA, MEXICO	6604	E	34.8	6.4	0.62	0.95
		N			0.58	1.78
WHITTIER NARROWS	14403	E	22.5	6	0.29	0.73
		N			0.39	2.62
LOMA PRIETA	58065	E	13	6.9	0.51	0.51
		N			0.32	2.95
NORTHRIDGE	90021	E	29	6.7	0.4	3.17
		N			0.36	2.65
NORTHRIDGE	24087	E	9.2	6.7	0.34	0.85
		N			0.3	1.46
CHI-CHI	TCU047	E	33.01	7.6	0.41	1.85
		N			0.3	0.88

In both directions of the building, the density of the walls was 5%. The reinforcement of the ties consisted of 4 steel bars 10 mm in diameter with a yielding strength of 300 Mpa. The compression strength of concrete was also assumed to be 15 Mpa. For example, the properties of the elements in the first story of a two-story CMS with a tensile strength for masonry equal to 0.25 MPa are shown in Table 1. Ensembles of seven earthquake ground motions in the form of two-component records (longitudinal and transverse components) were extracted from the PEER Strong Motion Database (Table 2).

The selected accelerograms had PGA values of 0.3 to 0.4 g and recorded a significant duration of least 10 s. These were recorded on a firm soil site (site classification B; USGS). This reflected the threatening conditions to which typical masonry construction was subjected because of the frequency content and high relative risk in the area (Ranjbaran and Hosseini 2014).

4. Calibration of parameters for displacement-based method

Sec. 2 demonstrates that to determine the displacement demand in a displacement-based seismic assessment approach, it is necessary to specify T_y as the yield period of vibration, $\boldsymbol{\alpha}$ as the ratio of the post stiffness to the initial stiffness, and ξ_{hyst}, as hysteretic damping of ESDOF. The prototype structure was analyzed in the form of nonlinear IDA with the records in Table 2. For IDA analysis at first all of the records were scaled to 1 g and then although the prototype structure failed beyond a PGA of 0.65 g in most cases (Ranjbaran and Hosseini 2014), the seven coupled records were scaled from PGA=0.1 g to PGA=1 g at increments of 0.1 and applied in the two directions of the model. Illogical results were then eliminated from the database. Each of CMW was modeled by an equivalent linear element with boundary conditions of pined in bottom and rolled- fixed in top of the element (Fig. 1(c)) and shear hinge at mid-span of element with constitutive behavior from proposed analytical model to simulate the in plane nonlinear behavior of CMW. With assumption rigid diaphragm in the ceiling the "rigidDiaphragm" command was used in the modeling at each level of story. Thin Takeda-type degrading stiffness model was employed using (β=0.25) to determine the degraded unloading stiffness based on ductility. The viscous damping by using the Rayleigh viscous matrix was obtained and the damping ratio was considered 5% (Flores and Alcocer 1996, Tomazevich and Klemenk 1997, Ranjbaran and Hosseini 2014).

4.1 Determination of T_y and α

The yield period of vibration of each building was estimated from a simplified Eq. (8) as

$$T_y = aH_T^b \tag{8}$$

where H_T is the total height of the actual building and a and b are coefficients defined for different types of buildings according to seismic assessment codes or were obtained using nonlinear dynamic time-history analysis.

These coefficients were calibrated herein using the second method.

After analysis, the base shear force and lateral displacement were obtained for the prototype structure by considering all uncertainty and scaled accelerograms. The data was converted to equivalent properties in terms of

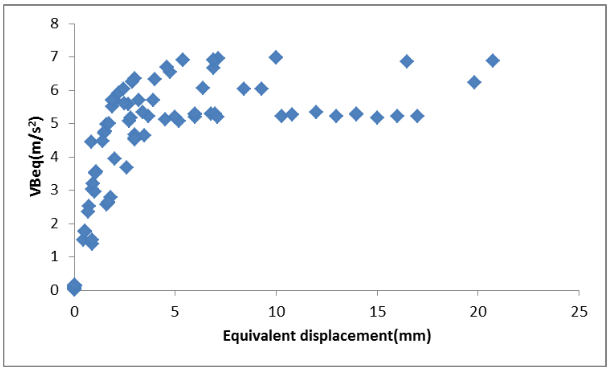

Fig. 8 Equivalent capacity curve for two-story building in two directions (f_t=0.25 MPa)

lateral force and displacement to represent the building response as an ESDOF system. Equivalent displacement and equivalent lateral force can be calculated using Eqs. (9) to (11) (Priestley *et al*. 2007, Ahamad *et al*. 2010) as

$$\Delta_{eq} = \frac{\sum_{i=1}^{n} M_i \Delta_i^2}{\sum_{i=1}^{n} M_i \Delta_i} \tag{9}$$

$$VB_{eq} = \frac{VB}{M_{eq}} \tag{10}$$

$$M_{eq} = \sum_{i=1}^{n} \frac{M_i \Delta_i}{\Delta_{eq}} \tag{11}$$

where M_i is the ith floor mass, *VB* is the maximum base shear force, and Δ_i is the maximum displacement demand of the ith floor of the prototype structure for a given accelerogram. VB_{eq} and Δ_{eq} were obtained for all accelograms by increasing the PGA and then deriving the equivalent capacity curve for the ESDOF system (Fig. 8). Only the pre-yield and yielding points of this curve were used for computation of the yield vibration period using Eq. (12)

$$T_y = 2\pi \sqrt{\Delta_{eq}/VB_{eq}} \tag{12}$$

This procedure was repeated for the prototype structure with all of the mechanical properties separated from the total height of the structure. Ensembles of data were plotted in the form of T_y (yield period vibration) versus *H* (height of CMS) (Fig. 9). Nonlinear regression was used to obtain values for coefficients *a* and *b* of 0.06 and 0.75, respectively.

Ahmad *et al*. (2010) obtained values for coefficients *a* and *b* of 0.05 and 0.75, respectively, for unconfined masonry structures. T_y was slightly over-estimated, which could be caused by the assumption of a low value for the masonry tensile strength within its range (0.04-0.25 MPa).

Fig. 9 shows that the dispersion of T_y is low for buildings with less height and high for buildings with greater height because of the increase in the DOF and a possible higher mode of participation.

Tomazevich (1999) proposed the range of tensile strength for a masonry to be 0.03 $f_m \le f_t \le 0.09$ f_m and the range of modules of elasticity to be 200 $f_m \le E_m \le 2000 f_m$ (f_m is the compressive strength of masonry) that resulted in illogically high values for the yield vibration period for low values of the modules of elasticity and vice versa. In the present paper, it appears that the range of 1000 $f_m \le E_m \le 1500 f_m$ is more logical for the relatively good details of construction of masonry structures.

Cyclic degradation decreases stiffness as demand increases in the constitutive behavior of CMS (Ranjbaran and Hosseini 2014). Factor $\boldsymbol{\alpha}$ was obtained by identification of the slope of the post-yield branch of the equivalent capacity curve for the ESDOF system (Fig. 8). The slope was computed for all cases where the CMS in each direction was calculated separately and then considered together to estimate the mean value. A mean value of zero was observed for all cases. It should be mentioned that this value was estimated to be -0.05 for unconfined masonry buildings (Ahamad *et al*. 2010).

4.2. Determination of ξ_{hyst}

The most common method for defining equivalent viscous damping resulting from hysteretic damping is to equate the energy dissipated in a vibration cycle of the inelastic system and the equivalent linear system (Dwairi et *al*. 2007, Chopra and Goel 1999). It can be shown that the equivalent viscous damping ratio was

$$\xi_{hyst} = \frac{1}{4\pi} \frac{E_D}{E_S} \tag{13}$$

where E_D is the energy dissipated in the inelastic system given by the area enclosed by the hysteresis loop and results from nonlinear dynamic analysis and E_S is the strain energy of the linear system with stiffness k_{sec} (Fig. 10).

It is possible to measure the energy dissipation in the prototype structure in terms of ductility (Eq. (5)) using the ESDOF system. The prototype structures with various properties and height were idealized using ESDOF and characterized with M_e, H_e and K_e. The hysteretic behavior was assigned to a shear hinge at mid-span of H_e (Fig. 11). H_e and M_e are defined in Eqs. (3) and (14) respectively (Lang 2002) as

$$\mathrm{M_e} = \sum \mathrm{m_i}\, \varphi_\mathrm{i} \tag{14}$$

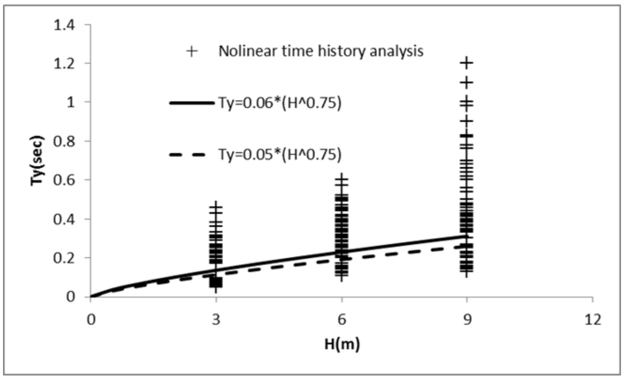

Fig. 9 Yield vibration period of prototype structure

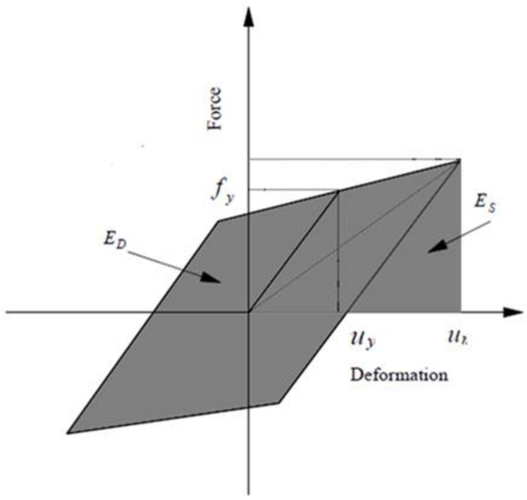

Fig. 10 Equivalent viscous damping caused by hysteretic energy dissipation (Chopra and Goel 1999)

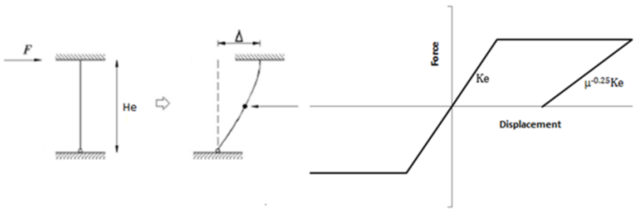

Fig. 11 ESDOF system for determination of equivalent viscous damping.

where m_i is the mass of the ith floor of the prototype structure and φ_i is the displacement amplitude of the ith floor of the fundamental mode shape normalized to have a unit value at the roof.

The capacity curves of the prototype structures were obtained from push-over analysis using lateral forces in proportion to the product of the mass and fundamental mode shape and were transformed to the force-displacement relationship of the ESDOF system.

Fig. 12 shows the capacity curve of a two-story building for which the tensile strength of the masonry equals 0.25 MPa in the *X* direction. Equivalent base shear V_e and equivalent displacement U_e of the ESDOF system were determined using the corresponding values for the prototype structure divided by the modal participation factor as shown in Eqs. (15) to (17) (Jeong and Elnashai 2007)

$$V_e = \frac{V}{\Gamma} \tag{15}$$

$$U_e = \frac{U}{\Gamma} \tag{16}$$

$$\Gamma = \frac{\sum \mathrm{m_i}\, \varphi_\mathrm{i}}{\sum \mathrm{m_i}\, \varphi_\mathrm{i}^2} \tag{17}$$

The transformed ESDOF capacity curve is in the form of perfectly-elastic plastic ($\boldsymbol{\alpha}$ = 0). To assign cyclic behavior to the ESDOF system for nonlinear dynamic analysis, a thin Takeda-type degrading stiffness model was employed using ($\boldsymbol{\beta}$ = 0.25) to determine the degraded unloading stiffness based on ductility (Fig. 11) (Ranjbaran and Hosseini 2014). The geometrical properties of the ESDOF system is defined in Eq. (18) as

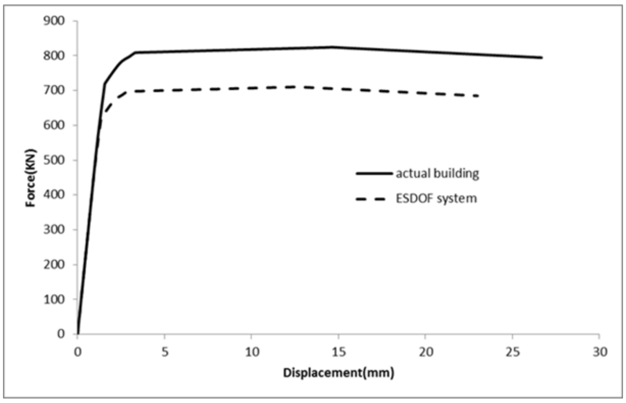

Fig. 12 Capacity curve of two-story building and its ESDOF system

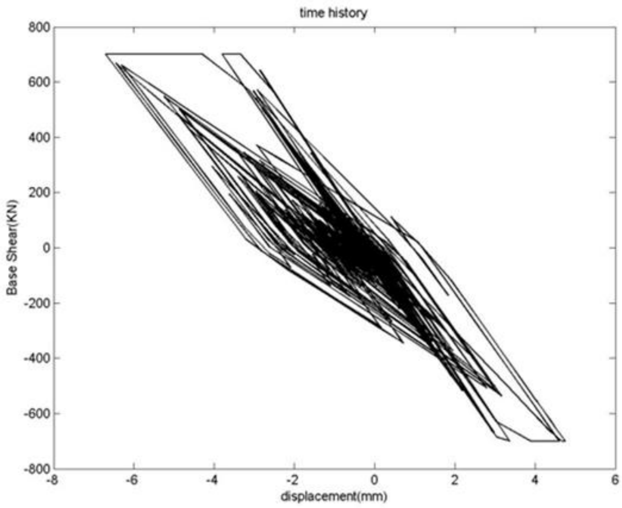

Fig. 13 Time-history response of base shear versus displacement

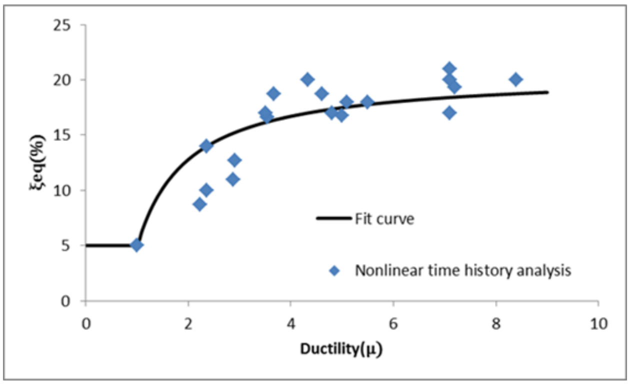

Fig. 14 Equivalent viscous damping in terms of ductility

$$K_e = \frac{3EI_e}{H_e^3} \tag{18}$$

Using nonlinear dynamic analysis of the ESDOF system through application of an assumed accelerogram, the response of the base shear versus displacement was

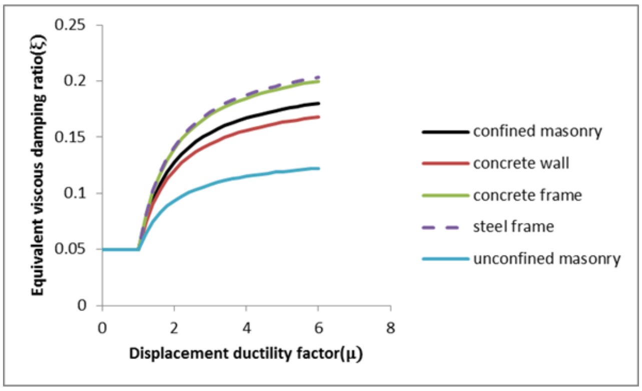

Fig. 15 Hysteretic damping of different structures

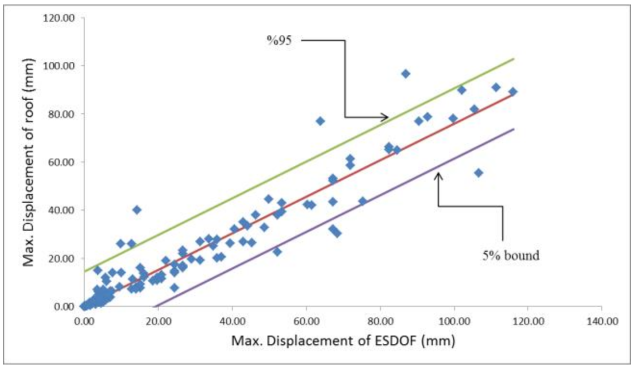

Fig. 16 Correlation between response of actual building and ESDOF system

achieved (Fig. 13). Nonlinear IDA of the ESDOF system and Eqs. (5) and (13) were then used to gather the dataset that represents ζ_{hyst} versus μ.

Eq. (7) and nonlinear regression in the form of Eq. (19) was carried out as recommended by Dwairi and Kowalsky (2007) and the value of parameter C was determined to be 0.49 (Fig. 14)

$$\xi_{eq}=0.05+C\left(\frac{\mu-1}{\mu\pi}\right) \tag{19}$$

Fig. 15 compares the equivalent viscous damping of a confined masonry building with other types of structures (Priestley *et al*. 2007). Hysteretic damping of CMS occurs near the concrete wall and is much greater than the unconfined masonry structures.

4.3 Response of ESDOF versus that of actual building

The uncertainty caused by simplification of the ESDOF approach was quantified by comparing the maximum displacement of the roof and ESDOF of the prototype structure resulting from nonlinear IDA analysis (Fig. 16). Based on this correlation, the following relation is suggested for use in identification of demand displacement in the proposed approach

$$\delta(\text{actual}) = 0.76 \times \delta(\text{ESDOF}) \tag{20}$$

The respective uncertainty (standard error of the estimate) in the prediction of the actual of displacement is 7.3 and the correlation coefficient of equation is R^2=0.9. Fig. 16 shows that the dispersion of data related to equation increases as the intensity of the ground motion increases. So it is expected that the precision of the proposed method could be decreased with increasing damage or limit state in CMS.

5. Case study

A two-story confined masonry structure located in a region of high seismicity (design acceleration of 0.35 g) on a firm site was modeled as a numerical example to verify the accuracy of the proposed method. This model is named "Simplified method" in this paper. The limit states were considered as displacement for yield (Δ_y) and maximum strength (Δ_u) with parameters as follows:

φ_1 =0.65, φ_2=1, h_1=3 m, h_2=6 m, $m_{1,2}$=69029 Nm/s^2, Me=113.89 KNm/s^2, H_e=4.8 m, Γ=1.16

For simplification, φ_i is considered proportional to the ratio of the height of the story. As stated in sec. 2, θ_y and θ_u were calibrated based on previous investigations by the authors (Ranjbaran and Hosseini 2014). The mean values of Δ_y and Δ_u of the two-story prototype structure was 4 and 24.3 mm, respectively, making the value of Δ_y for ESDOF system 3.45 and θ_y equal to 0.072%. Fig. 5 shows that the value of θ_y corresponds to a 90% probability of failure, which also corresponds to the maximum strength drift ratio of 0.66%. This results in a maximum strength displacement of the ESDOF system of 21.1 mm and for an actual building of 24.5 mm. It appears that the allocation of values of θ_y and θ_u as equivalent to 7.2e-4 and 6.6e-3 is logical. The properties of the accelerograms used are presented as Table 3 and the calculated values corresponding to the limit states are as follows:

θ_y = 7.2e-4, θ_u =6.6e-3, Δ_y =3.45 mm, Δ_u =21.1 mm, μ_{LS} =6.11, T_y=0.23 sec, T_{LS}=0.57 sec, ξ_{eq}=0.18, η=0.6

Table 3 Properties of used earthquakes

Earthquake	Direction	r (km)	Mw	PGA (g)	δmax (mm)	Tc (sec)
Sanfernando	*x*	24.2	6.6	0.32	100.87	3.25
	y	24.2	6.6	0.26	100.87	3.25
Victoria	*x*	34.8	6.4	0.62	45.54	2.75
	y	34.8	6.4	0.58	45.54	2.75
Whittier	*x*	22.5	6	0.29	28.04	1.75
	y	22.5	6	0.39	28.04	1.75
Lomaprieta	*x*	13	6.9	0.51	385.52	4
	y	13	6.9	0.32	385.52	4
Northridge	*x*	29	6.7	0.4	109.04	3.5
	y	29	6.7	0.36	109.04	3.5
Northridge	*x*	9.2	6.7	0.34	343.72	3.5
	y	9.2	6.7	0.3	343.72	3.5
Chi-Chi	*x*	33.01	7.6	0.41	760.94	5.75
	y	33.01	7.6	0.3	760.94	5.75

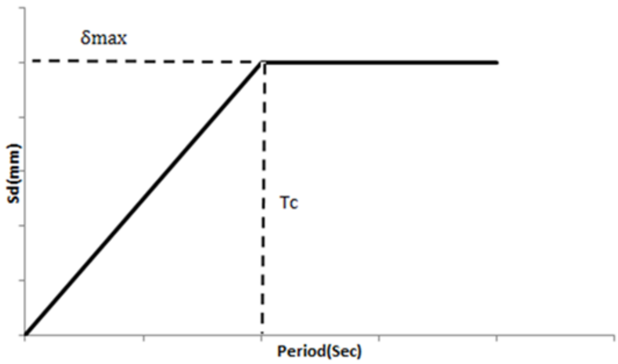

Fig. 17 General form of elastic displacement spectra (Priestley *et al*. 2007)

The general form of the elastic displacement response spectra could be considered as shown in Fig. 17 (Priestley *et al*. 2007) as

$$\delta_{\max} = C_s \times \frac{10^{(M_w-3.2)}}{r} \mathrm{mm} \tag{21}$$

$$T_c = 1 + 2.5(M_w - 5.7)\mathrm{sec} \tag{22}$$

where r (km) and M_w are the closest distances to fault rupture and the magnitude of the earthquake, respectively and C_s depends on the site effect as follows:

rock: C_s=0.7

firm ground: C_s=1

intermediate soil: C_s=1.4

very soft soil: C_s=1.8

Previously a study was conducted on the two-story confined masonry buildings located on the firm ground by author that a series of pushover analysis were performed to obtain damage indices and a series of nonlinear incremental dynamic analysis (IDA) were conducted to identify the seismic demand (Ranjbaran and Hosseini 2014). The plan of these buildings, the range of mechanical parameters of masonry walls and accelerograms were the same as plan, parameters and accelerograms in this paper. As indicated in Fig. 19, the mean values of maximum displacement response of roof from a series of inelastic dynamic analysis can be plotted against PGA and a forth order polynomial regression function that represents the mean of the maximum displacement demand as a function of the PGA is used for deriving fragility curves based on PGA. Finally by considering various, the fragility curves with assuming a log normal distribution of data were derived based on capacity and demand of CMSs in a probabilistic approach. In this paper the results of that study are named "Analytical method" to compare with the results of the simplified method. As it was mentioned the used records in the analytical method with characteristics in Table 3 are applied for numerical example of the simplified method. For example, $\delta_{\max}$ and T_c for the Chi-Chi and Northridge earthquakes are 760.94 mm, 5.75 s and 109.04 mm, 3.5 s, respectively. The inelastic displacement response spectra corresponding to the maximum strength limit state assuming a PGA of 0.25 g was determined by multiplying $\delta_{\max}$ by η and scaling the PGA as:

Chi-Chi: $\frac{0.25}{0.3} \times 0.6 \times 760.94 = 379.21$ mm

Northridge: $\frac{0.25}{0.4} \times 0.6 \times 109.04 = 40.78$ mm

The demand displacement for T=0.57 s with a calibration factor of 0.76 for the Chi-Chi and Northridge earthquakes are 28.56 and 5.04 mm, respectively.

Chi-Chi: $28.56 > 21.1 \rightarrow$ vulnerable

Northridge: $5.04 < 21.1 \rightarrow$ not vulnerable

The fragility curves are obtained by using lognormal probability paper (Fig. 18) (Boreckci and Kircil 2011).In this investigation the parameters of distribution λ and ζ (mean and standard deviation) for limit states of LS1 and LS2 are presented in Table 4.

As it is shown in Fig. 18 and stated previously the results of the simplified method corresponding to limit state of LS1 is more near the analytical method rather than limit state of LS2.The results of simplified method for limit states of LS1&LS2 after ground motion intensity of 0.25 and 0.8 g respectively are underestimated and have less difference with respect to the analytical method. These intensity values are corresponding to elastic and maximum strength of confined masonry building according to experimental (Tomazevic and Klemenc 1997) and numerical studies

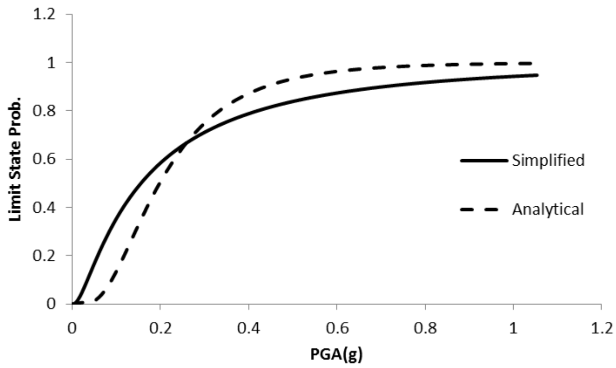

(a)

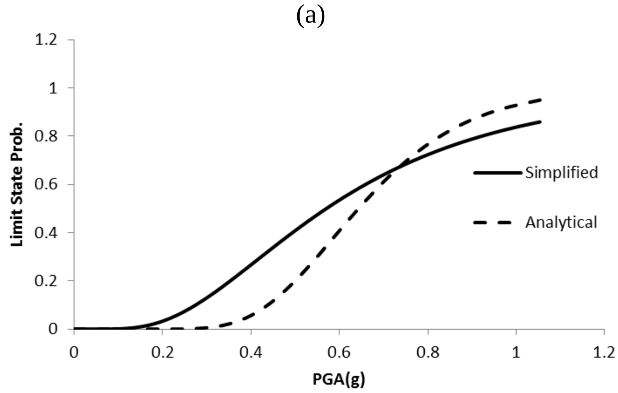

(b)

Fig. 18 Fragility curves of CMS using simplified and analytical method: (a) LS1 limit state; (b) LS2 limit state

Table 4 The parameters of fragility curves

	LS1		LS2	
	λ	ζ	λ	ζ
Analytical	7.57	0.62	8.75	0.3
Simplified	7.33	1.18	8.63	0.57

(Ranjbaran and Hosseini 2014). In Fig. 19 and Table 5 the values of mean of maximum displacement of roof caused by the analytical and simplified method are compared with each other. It seems with increasing damage in CMS (LS2 limit state) the precision of proposed simplified method decreases. The precision of proposed method depends on the precision of the estimated displacement demand, as it is stated previously by increasing intensity of ground motion or damage state the correlation between the analytical and simplified displacement decreases (Eq. (20)) and the estimated parameters of ESDOF in each limit state depends on the intensity ground motion resulted in that of the limit state.

The effect of number story in the simplified method is shown in the Fig. 20. The used previous records for 2 stories CMS are used for 1 story CMS with the same properties. As it is shown the difference between them is low. The calculated values corresponding to the limit states are as follows:

θ_y= 7.2e-4, θ_u =6.6e-3, Δ_y=2.16 mm, Δ_u=19.8 mm,
μ_{LS} =9.17, T_y=0.14 sec, T_{LS}=0.41 sec ξ_{eq}=0.19, η=0.58

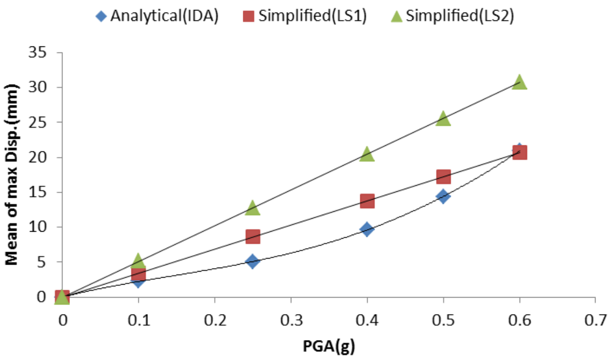

Fig. 19 Comparison between results of analytical and simplified method

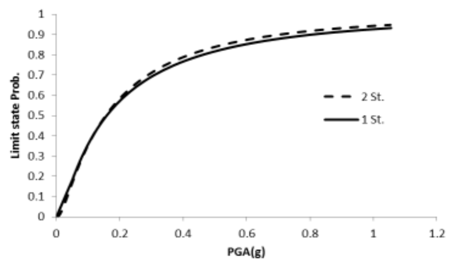

(a)

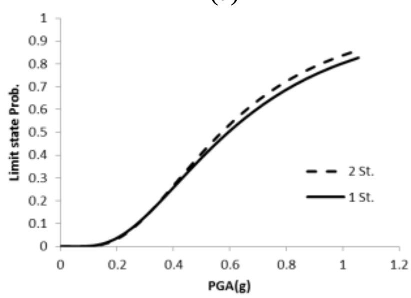

(b)

Fig. 20 The Fragility curves in 1&2 stories CMS based on simplified method, a) LS1 limit state, b) LS2 limit state

Table 5 Comparison of mean of maximum displacement of roof in simplified and analytical method

PGA (g)	Analytical (mm)	Simplified (mm)		S/A	
		LS1	LS2	LS1	LS2
0.1	2.25	3.44	5.12	1.53	2.27
0.25	5.04	8.60	12.79	1.71	2.54
0.4	9.68	13.76	20.46	1.42	2.11
0.5	14.36	17.20	25.58	1.20	1.78
0.6	20.94	20.64	30.70	0.99	1.47

6. Conclusions

A simplified method was presented for seismic vulnerability assessment of confined masonry structures based on displacement. The ratio of demand and capacity displacement (DCR) of the equivalent single degree of freedom (ESDOF) system, which correspond to an actual building, were compared. When DCR>1, the building should be considered vulnerable and when DCR<1, it should be considered invulnerable. The demand displacement is determined based on nonlinear displacement spectra for the specified limit state, and the capacity displacement is determined based on the capacity of drift corresponded to that of the specified limit state. The proposed method is precise in its simplicity. This method is especially useful for hazard analysis of earthquake-prone areas having a considerable number of confined masonry buildings. The results of the proposed method were compared with those from the analytical method and it seems with increasing damage in CMS the precision of proposed simplified method decreases.

Reference

Ahamad, N., Crowley, H., Pinho, R. and Ali, Q. (2010), "Displacement-based earthquake loss assessment of masonry buildings in Mansehra City, Pakistan", *J. Earthq. Eng.*, **14**(S1), 1-37.

Alcocer, S.M., Ruiz, J., Pineda, A. and Zepeda, A. (1996), "Retrofitting of confined masonry walls with welded wire mesh", *Eleventh world conference on earthquake engineering*, paper No 1471.

Boreckci, M. and Kircil, M. (2011), "Fragility analysis of R/C frame buildings based on different types of hysteretic model", *Struct. Eng. Mech.*, **39**(6), 795-812.

Brzev, S. (2007), Earthquake-Resistant confined masonry construction, National information center of earthquake engineering(NICEE).

Comite Europeen de Normalisation (CEN) Eurocode 8. (1994), Design Provisions for Earthquake Resistance of Structures, Part 1-1: General Rules-Seismic Actions and General Requirements for Structures, prEN 1998-1-1, CEN, Belgium.

Chopra, A. and Goel, R. (1999), "Capacity-demand-diagram methods for estimating seismic deformation of inelastic structures: SDF systems", *Civ. Environ. Eng.*, 53.

Chopra, A. and Goel, R. (2001), "Direct displacement-based design use of inelastic vs. elastic design spectra", *Earthq. Spectra*, **17**(1), 47-64.

Design code (2011), *Seismic Design guide for low rise confined masonry buildings*, Okland, California.

DIANA (2005), "DIANA finite element analysis, user's manual-element library", Delft: TNO Building and Construction Research.

Dwairi, H.M., Kowalsky, M.J. and Nau, J.M. (2007), "Equivalent damping in support of direct displacement-based design", *J. Earthq. Eng.*, **11**(4), 512-530.

Flores, L.E. and Alcocer, S.M. (1996), "Calculated response of confined masonry structures", *11th World conference on Earthquake Engineering*, Paper No. 1830.

Jeong, S.H. and Elnashai, A. (2007), "Probabilistic fragility analysis parameterized by fundamental response quantities", *Eng. Struct.*, **29**(6), 1238-1251.

Lang, K. (2002), *Seismic vulnerability of existing buildings. Institute of structural Engineering*, Swiss Federal Institute of Technology Zurich.

Lourenco, P. (1996), "Computational strategies for masonry structures", Delft university.

Marinilli, A. and Castilla, E. (2004), "Experimental evaluation of confined masonry walls with several confining columns", *Proceedings of the Thirteenth World Conference on Earthquake Engineering*, Vancouver, Canada, August.

Moroni, M.O., Astroza, M. and Tavonatti, S. (1994), "Nonlinear models for shear failure in confined masonry walls", *The Masonry Soc. J.*, **12**(2), 72-77.

OpenSees (2006), "OpenSees command language manual, Pacific, Earthquake engineering research center", University of California, Berkeley,

OpenSees (2009), "Open System for Earthquake Engineering Simulation: OpenSees v2.3.2", http//:opensees.berkeley.edu.

Priestley, M.J.N. (1997), "Displacement-based seismic assessment of reinforced concrete buildings", *J. Earthq. Eng.*, **1**(1), 157-192.

Priestley, M.J.N, Calvi, G.M. and Kowalsky, M.J. (2007), "Displacement-based seismic design of structures", IUSS Press.

Ranjbaran, F. and Hosseini, M. (2010), "A Simplified behavioral model for nonlinear seismic analysis of confined masonry walls", *Proceedings of the 9th US National and 10th Canadian Conference on Earthquake Engineering*, Toronto, Ontario, Canada.

Ranjbaran, F., Hosseini, M. and Soltani, S. (2012), "Simplified formulation for modeling the nonlinear behavior of confined masonry walls in seismic analysis", *Int. J. Architec. Herit.*, **6**(3), 259-289.

Ranjbaran, F. and Hosseini, M. (2014), "Seismic vulnerability assessment of confined masonry wall buildings", *Earthq. Struct.*, **7**(2), 201-216.

Riahi, Z., Elwood, K. and Alcocer, S.M. (2009), "Backbone model for confined masonry walls for performance -based seismic design", *J. Struct. Eng*., ASCE, **135**(6), 644-654.

Ruiz-Garcia, J. and Negrete, M. (2009), "Drift-based fragility assessment of confined masonry walls in seismic zones", *Eng Struct.*, **31**(1), 170-181.

Ruiz-Garcia, J. and Negrete, M. (2009), "A simplified drift-based assessment procedure for regular confined masonry buildings in seismic regions", *J. Earthq. Eng.*, **13**(4), 520-539.

Shibata, A. and Sozen, M.A. (1976), "Substitute-structure method for seismic design in R/C", *J. Struct. Div.*, ASCE, **102**, 1-18.

Teran-Gilmore, A., Zuniga-Cuevas, O.A. and Ruiz-Garcia, J. (2009), "Displacement-based assessment of low-height confined masonry buildings", *Earthq. Spectra*, **25**(2), 439-464.

Tomazevich, M. and Klemenk, I. (1997), "Verification of seismic resistance of confined masonry buildings", *Earthq. Eng. Struct. Dyn*., **26**(10), 1073-1088.

Tomazevic, M. and Klemenc, I. (1998), "Seismic behavior of confined masonry walls", *Earthq. Eng. Struct. Dyn.*, **26**(10), 1059-1071.

Tomazevic, M. (1999), *Earthquake Resistant design of masonry buildings*, Imperial college press.

CC